Am J Cancer Res 2023;13(12):5966-5980
www.ajcr.us /ISSN:2156-6976/ajcr0153509

Original Article

Poliovirus receptor inhibition in breast cancer cells induces antitumor immunity via T cell activation

Kyung-Hee Song[1], Seung-Youn Jung[1], Jeong-In Park[1], Dong-Hyeon Lee[1], Jiyeon Ahn[1], Sang-Gu Hwang[1], Dae-Seog Lim[2], Jie-Young Song[1]

[1]*Division of Radiation Biomedical Research, Korea Institute of Radiological and Medical Sciences, Seoul 01812, Republic of Korea;* [2]*Department of Biotechnology, CHA University, Gyeonggi-do 13488, Republic of Korea*

Received September 19, 2023; Accepted December 2, 2023; Epub December 15, 2023; Published December 30, 2023

Abstract: Radiotherapy (RT) is a commonly used treatment option for patients with cancer because it can effectively control tumor growth and kill tumor cells. However, the impact of RT goes beyond direct tumor cell killing because it can change the tumor microenvironment by altering surrounding tissues and infiltrating cells and modulating the expression of immune checkpoints. Poliovirus receptor (PVR, cluster of differentiation (CD)155), a member of the nectin-like molecule family, is overexpressed in many human cancers. However, its role in the tumor growth and T-cell immune responses of triple-negative breast cancer (TNBC) remains unclear. In the present study, we observe that radiation exposure increases PVR expression in MDA-MB-231 and BT549 cells. Silencing PVR not only inhibited the proliferation of breast cancer cells but also significantly enhanced the cytotoxicity of cytotoxic T lymphocytes (CTLs) compared with the control or RT groups. Treatment of T cells with PVR decreased $CD8^+$ T cells, increased $CD4^+$ T cells, and induced PVR ligands such as T cell immunoreceptor with immunoglobulin and ITIM domain, CD226, and CD96. However, after treatment with PVR, CTL responses decreased and secretion of interferon-γ, tumor necrosis factor-α, interleukin (IL)-2, IL-6, and IL-10 was significantly inhibited. In contrast, PVR knockdown increased the production of these cytokines, illustrating the immunosuppressive function of PVR. Suppression of PVR using an anti-PVR antibody inhibited 4T1 tumor growth by increasing immune cell infiltration. These results provide new insights into the role of PVR in TNBC and highlight its potential as a target for T cell-mediated immunotherapy in breast cancer.

Keywords: Radiotherapy, tumor microenvironment, immune checkpoint, antitumor immunity, cytotoxic T cells

Introduction

Radiotherapy (RT) is the most common therapeutic modality for cancers; however, some patients develop radioresistance and recurrence, resulting in poor prognosis and reduced overall survival (OS) [1, 2]. RT success primarily depends on its ability to induce tumor cell death. In addition, RT can change the tumor microenvironment (TME) by altering surrounding tissues and infiltrating cells and modulating the expression of immune checkpoints (ICs) [3, 4]. Depending on the balance between RT-induced pro- and antitumor immune responses, these changes either promote or inhibit tumor growth.

In early RT stages, dying cells actively or passively release damage-associated molecular patterns and tumor-associated antigens, activating innate immune cells, including dendritic cells (DCs), macrophages, and natural killer (NK) cells. These immune cells can prime and activate cytotoxic T lymphocytes (CTLs) and other effector T cells, resulting in a robust antitumor immune response [5]. This initiates "immune recognition" between dying cancer cells and the immune system. RT-induced T cell cross-priming depends on immunogenic cell death molecular signal activation and requires interferon (IFN) I production by tumor-infiltrating cells [6]. However, tumor elimination by RT-activated immunity also triggers immunosuppressive mechanisms, limiting the antitumor effects of RT. For example, RT induces the expression of potent proinflammatory cytokines such as IFN I and II. These cytokines can induce the expression of programmed death-ligand 1

(PD-L1) [7]. Studies have indicated that radiation induces PD-L1 upregulation in the TME, mediating radioresistance [8, 9]. These findings form the basis for several trials that combine RT with PD-1/PD-L1 checkpoint inhibition.

As natural regulators of the immune system, IC proteins prevent excessive immune responses and maintain immune homeostasis [10]. Recently, many immune inhibitory receptors have been identified and studied in cancer, including PD-1, CTL-associated antigen 4, lymphocyte-activation gene 3, T-cell immunoglobulin and mucin-domain containing-3, T-cell immunoglobulin and ITIM domain (TIGIT), and B and T lymphocyte attenuator. The interaction of these receptors with their ligands on cancer or other cells in the TME can lead to T cell function inhibition and contribute to tumor immune evasion. Anti-PD-1/PD-L1 therapy is the most successful IC blockade therapy approved to treat various cancer types, including blood, skin, lung, liver, bladder, and kidney cancers [10, 11].

Herein, we specifically focused on the upregulation of ICs expressed on tumors after radiation. Poliovirus receptor (PVR, cluster of differentiation (CD)155) was highly increased by radiation. PVR plays a vital role in various biological processes, including cell growth, invasion, migration, and adhesion and immunomodulatory responses during malignancy development [12-15]. PVR expression is significantly upregulated in most human cancers and is highly correlated with poor prognosis [16-18]. Recent studies have identified PVR as a ligand for T and NK cell-expressed receptors. PVR has been recognized as a promising immunotherapy target because it can bind to both the costimulatory immune receptor CD226 and inhibitory checkpoint receptors TIGIT and Tactile (CD96) [19-21]. However, the exact mechanisms of PVR's effect on tumor progression and T cell responses remain unknown.

In this study, using breast cancer cells, we elucidated the expression and prognostic value of PVR after RT and determined the interaction between PVR and T-cell function. Targeting PVR that is capable of reinvigorating T cells in the TME may be a novel therapeutic alternative for patients with breast cancer.

Materials and methods

Cell lines and culture

The human triple negative breast cancer (TNBC) cell lines, BT549 and MDA-MB-231, and the murine mammary tumor cell line 4T1 were obtained from American Type Culture Collection (Manassas, VA, USA). These cells were cultured in RPMI1640 medium (Welgene, Gyengsangbuk-do, Korea) supplemented with 10% fetal bovine serum and 100 U/mL penicillin/streptomycin (Welgene) at 37°C under a 5% CO_2 atmosphere.

Cell transfection and irradiation

PVR was knocked down using 21-base siRNA duplexes (Bioneer, Daejeon, Korea). The siRNA sequences were as follows: siPVR#1, sense 5'-GAGGUAUCCAUCUCUGGCUAU-3' and antisense 5'-AUAGCCAGAGAUGGAUACCUC-3', siPVR#2, sense 5'-CGGCAAGAAUGUGACCUGCAA-3' and antisense 5'-UUGCAGGUCACAUUCUUGCCG-3', siPVR#3, sense 5'-GCCUGUAAUCCCAGCUUUA-3' and antisense 5'-UUGCAGGUCACAUUCUUGCCG-3'. Among these sequences, siPVR#2 demonstrated strong inhibition of PVR levels by RT-PCR analysis, and was used in subsequent experiments. Unless otherwise stated, siPVR indicates siPVR#2. Nontargeting siRNA (Bioneer) was used as a negative control. RNAiMAX (Invitrogen, Waltham, MA, USA) was used according to the manufacturer's instructions to transfect subconfluent tumor cell lines with the siRNA duplexes. The cells were exposed to various radiation doses using ^{137}Cs γ-source Biobeam 8000 irradiator (Gamma-Service Medical GmbH, Leipzig, Germany) at a dose rate of 3.5 Gy/min.

Isolation of activated human CD3$^+$ T cells from peripheral blood mononuclear cells (PBMCs)

Human PBMCs were purchased from STEMCELL Technologies (#70025, Vancouver, BC, Canada) and cultured at 10^6 cells/mL in ImmnoCult™-XF T cell Expansion medium (#10981) containing human CD3/CD28 activator (#10991) according to the manufacturer's instructions. Cells were stimulated with 200 IU/mL IL-2 (PeproTech Rocky Hill, NJ, USA) every 3 days and cultured for 14 days. On day 14, human naïve CD3$^+$ T cells were purified using the EasySep™ Human

T cell enrichment isolation kit (#17951). A purity of approximately 97% was achieved.

Bioinformatics analysis

The Cancer Genome Atlas (TCGA) data were analyzed using UALCAN (ualcan.path.uab.edu/analysis.html). *PVR* mRNA expression in breast cancer based on OS was analyzed using GEPIA2 (gepia2.cancer-pku.cn/#index).

Clonogenic assay

Cells were seeded on 60-mm tissue culture dishes at various densities and then treated with different radiation doses. After 12-14 days, colonies were stained with 1% methylene blue (Sigma-Aldrich, St. Louis, MO, USA) solution in absolute methanol for 10 min. Colonies >0.1 mm in diameter were scored as surviving colonies.

Cell viability assay

Cells were seeded into 96-well plates (1×10^3 cells/well) and treated with 2 and 5 nM PVR siRNA for 6 h. Then, the cells were irradiated at 12 Gy for 24-72 h. After the treatment, cell viability was determined by measuring the mitochondrial conversion of MTT (5 mg/mL, Sigma-Aldrich) to formazan at an absorbance of 550 nm using a microplate reader (Multiskan EX, Thermo Fisher Scientific, Waltham, USA).

Flow cytometry

Immunostaining was performed as previously described [22]. Briefly, cells were incubated with human BD Fc Block™ (#564219, BD Biosciences, San Diego, CA, USA) and then stained with the corresponding antibodies. The antibodies used were as follows: CD155-APC (SKII.4), TIGIT-APC (A15153G), CD226-FITC (11A8), and CD96-APC (NK92.39) (BioLegend, San Diego, CA, USA). Naïve $CD3^+$ T cell differentiation was assessed via intracellular staining using a BD kit (BD Biosciences) according to the manufacturer's instructions. Cells were incubated with the BD GolgiStop™ Protein Transport Inhibitor for 4 h and stained with surface markers against CD3-FITC (HIT3a), CD4-APC (RPA-T4), CD4-FITC (RPA-T4), CD8-APC (SK1), and CD25-APC (M-A251). The cells were then permeabilized using a fixation/permeabilization solution (BD Biosciences) and stained with the following intracellular markers according to the manufacturer's instructions: IFNγ-FITC (B27), IL4-FITC (MP4-25D2), CD217-APC (W15177A), perforin-FITC (δG9), Foxp3-PE (259D) (all from BioLegend), and granzyme B-FITC (GB11, BD Biosciences). Stained cells were obtained using the CyFlow® Cube6 flow cytometer (Sysmex-Partec GmbH, Görlizt, Germany) and analyzed using FlowJo software (v.10, Tree Star, Ashland, OR, USA).

Cytotoxicity assay

The CytoTox 96 Nonradioactive Cytotoxicity assay (Promega, Madison, WI, USA) was used to determine specific cytotoxicity based on the colorimetric detection of released lactate dehydrogenase (LDH). Target cells were harvested, washed, counted, and diluted to 1×10^5 cells/mL. Then, 50 μL/well was added to 96-well plates. Effector $CD3^+$ T cells were added at effector-target cell ratios of 1:1, 5:1, 10:1, and 20:1 and co-cultured for 6 h. All conditions were assayed in quadruplicate. After incubating for 4 h at 37°C, LDH activity was determined using 50 μL of supernatant according to the manufacturer's instructions.

Western blotting

Western blotting was performed as described previously [23] using a specific antibody against PVR (81254S, Cell Signaling Technology, Danvers, MA, USA). β-actin (A5316, Sigma-Aldrich) was used for normalization. The optical density of each band was analyzed using Multi-Gauge v3 (Fujifilm, Tokyo, Japan).

Enzyme-linked immunosorbent assay (ELISA)

Cytokine levels in the supernatant were determined using ELISA kits for IFN-γ (#555142), tumor necrosis factor (TNF)-α (#555212), IL-2 (#555190), IL-6 (#555220), and IL-10 (#555157) according to the manufacturer's instructions (BD Biosciences).

In vivo studies using a syngeneic mouse model

Six-week-old female BALB/c mice were purchased from DooYeol Biotech (Seoul, Korea) and maintained under specific pathogen-free conditions. 4T1 cells (5×10^5 cells/100 μL phosphate-buffered saline) were subcutaneously injected into the right thigh. The mice

were randomly selected and locally irradiated once with high-dose radiation (8 Gy) using an X-ray irradiator (dose rate 2 Gy/min), and anti-PVR antibody (30 μg/mouse, BioLegend, #942104) or Rat IgG2a λ isotype control (BioLegend, #402302) was intratumorally administered for three days. Tumor volume was calculated 4-5 times per week after tumor administration using three orthogonal planes ($V = (L \times W \times W)/2$, where V is tumor volume, L is tumor length, and W is tumor width). Body weights from each group were measured 2-3 times per week. The animal experiments were performed according to our Institutional Animal Care and Use Committee, approved by the Korea Institute of Radiological & Medical Sciences (KIRAMS 2022-0139).

Isolation and phenotypic analysis of splenocytes and tumor-infiltrating lymphocytes (TILs)

The mice were euthanized, and their spleens were harvested 20 days after tumor cell injection. Isolated splenocytes were subjected to immunostaining as previously described [24]. For TIL isolation, tumors were cut into small pieces, resuspended in RPMI 1640 medium with 500 μL collagenase/hyaluronidase solution (STEMCELL Technologies, #07912) and 150 μg/mL DNase I solution (STEMCELL Technologies, #07900), and incubated for 25 min at 37°C with shaking. The digested samples were passed through a 70 μm nylon cell strainer to obtain a single-cell suspension. The cells were stained with the following monoclonal antibodies; TCRβ-APC (H57-597), CD11c-APC (HL3), CD44-FITC (IM7), CD19-FITC (1D3), CD80-FITC (16-10A1), and CD86-FITC (GL1) purchased from BD Biosciences; and CD4-APC (RM4-5), CD8a-APC (53-6.7), B220-APC (RA3-6B2), NK1.1-FITC (PK136), CD28-APC (37.51), CD25-APC (PC61), CD69-FITC (H1.2F3), F4/80-APC (BM8), and CD11b-FITC (M1/70) purchased from BioLegend. The results were analyzed using FlowJo software (v.10, FlowJo).

Statistical analysis

GraphPad Prism software version 8 (GraphPad, La Jolla, CA, USA) was used to perform statistical analyses. All data are expressed as mean ± standard error of mean. Analysis of variance and Tukey's post-hoc test were performed to determine significant between-group differences.

Results

Radiation increases PVR expression in human breast cancer cells

Based on the strong correlation between high PVR expression in cancer cells and resistance to anticancer therapy, we speculated that radiation-induced PVR expression reduces RT efficacy [19, 25, 26]. **Figure 1A** demonstrates that *PVR* mRNA expression was higher in the most aggressive TNBC type than in the other breast cancer subtypes (P = 1.68E-12). Furthermore, GEPIA2 analysis revealed a significant association between high PVR expression and shorter OS (HR = 1.9, P = 0.00022; **Figure 1B**). Therefore, MDA-MB-231 and BT549 cells were treated with the indicated radiation doses, followed by PVR expression measurement via flow cytometry and western blotting. Radiation significantly and dose-dependently increased PVR expression in both TNBC cell lines (**Figure 1C** and **1D**). However, the magnitude and persistence of PVR upregulation differed between the two cell lines; a higher response was observed in MDA-MB-231 cells than in BT549 cells. The clonogenic survival assay, to measure intrinsic radiosensitivity, revealed that MDA-MB-231 cells were more radioresistant than BT549 cells (**Figure 1E**). These results suggest that ionizing radiation (IR) significantly upregulates PVR expression in breast cancer cells and that PVR plays a critical role in acquiring radioresistance.

PVR inhibition increases CTL-mediated cytotoxicity

To explore the molecular mechanism underlying radiation-induced PVR upregulation, we used a siRNA targeting *PVR* (siPVR) to suppress PVR expression in the presence or absence of radiation. siPVR effectively suppressed PVR expression in both breast cancer cell lines, persisting for 48 h (**Figure 2A**). Furthermore, PVR protein levels decreased in cell lysates (**Figure 2B**). However, *PVR* knockdown alone or combined with IR had no significant effect on cancer cell viability, except for high-dose siPVR treatment 3 days after IR (**Figure 2C**). Another siRNA sequence (siPVR#1) also effectively reduced PVR expression up to 48 h post-irradiation without altering cell viability (Supplementary Figure 1A-C). To investigate PVR func-

PVR knockdown increases T cell activity

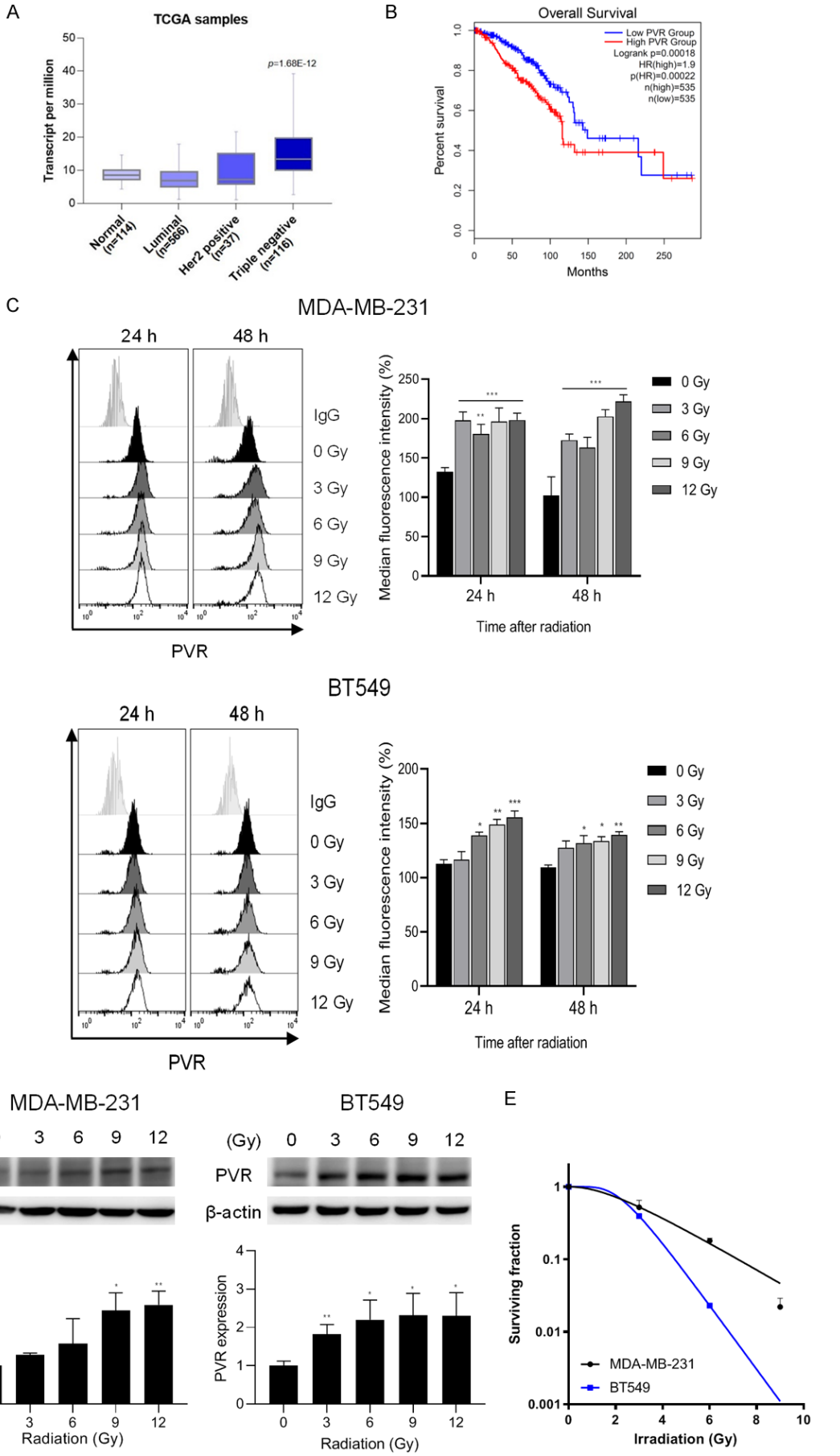

Figure 1. PVR expression in irradiated human breast cancer cells. A. Graphical overview of PVR mRNA expression in breast cancer (BRCA) subclasses was analyzed using UALCAN and TCGA BRCA dataset. B. Effects of PVR on the overall survival of patients with BRCA. The image with the highest logrank *p*-value is shown. C. Flow cytometry showing PVR levels in MDA-MB-231 and BT549 cells at the indicated time points after exposure to various IR doses. D. After 24 h of IR, western blotting was performed to measure PVR protein levels. E. Clonogenic survival fraction of cells was obtained at the indicated radiation exposures. Results are presented as mean ± SEM from three independent experiments. $^{*}P<0.05$, $^{**}P<0.01$, $^{***}P<0.001$ vs. 0 Gy control.

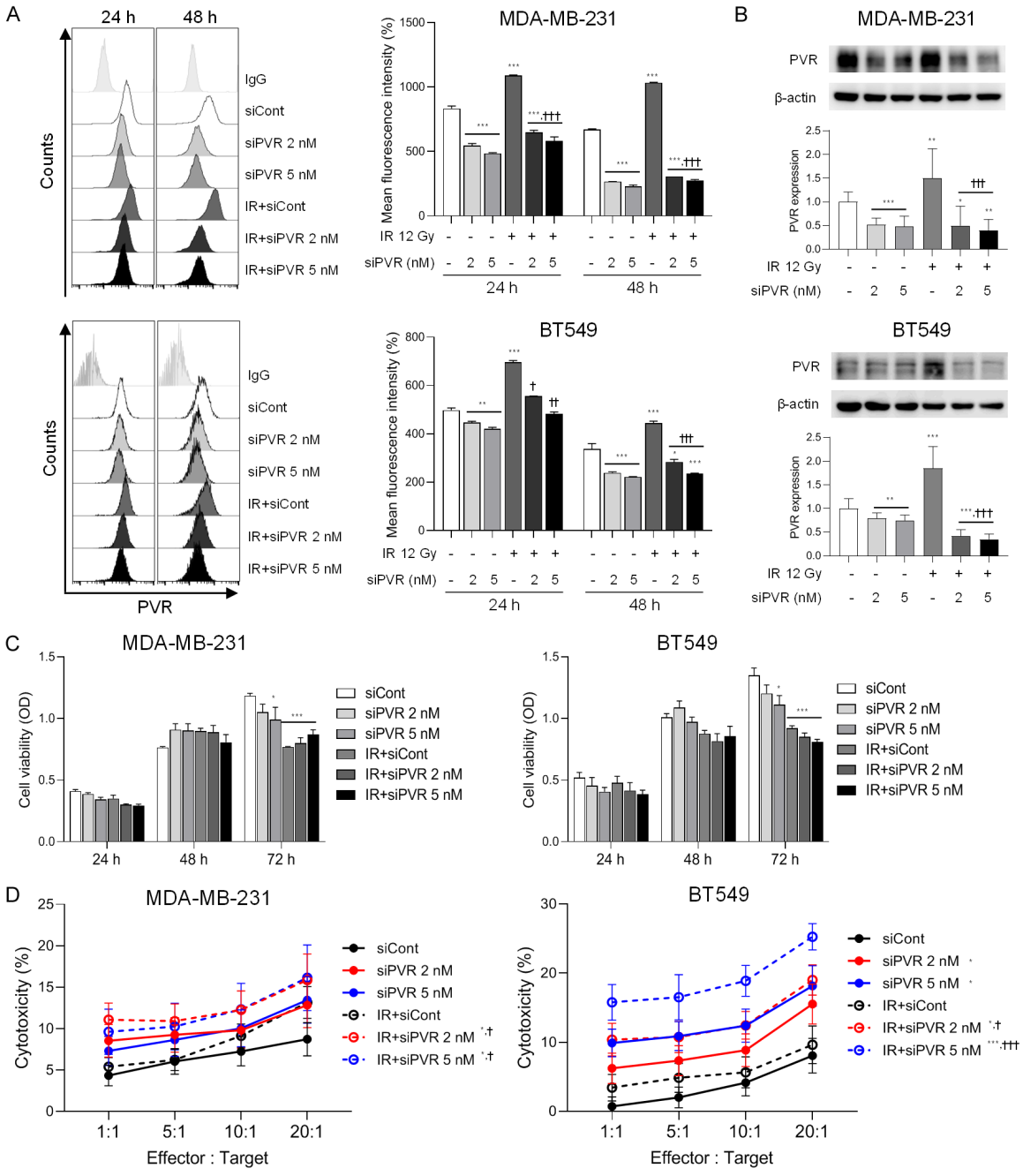

Figure 2. Effect of CTL responses on PVR depletion in irradiated breast cancer cells. Breast cancer cells were transfected with siPVR (2 and 5 nM) for 6 h and then irradiated. PVR expression was determined at indicated times after IR using (A) flow cytometry and (B) western blotting. (C) Cell viability was examined using the MTT assay. (D) CTL-mediated breast cancer cell killing was measured using the nonradioactive LDH assay. Results are presented as mean ± SEM from three independent experiments. $^{*}P<0.05$, $^{**}P<0.01$, $^{***}P<0.001$ vs. 0 Gy siCont, $^{\dagger}P<0.05$, $^{\dagger\dagger}P<0.01$, $^{\dagger\dagger\dagger}P<0.001$ vs. IR.

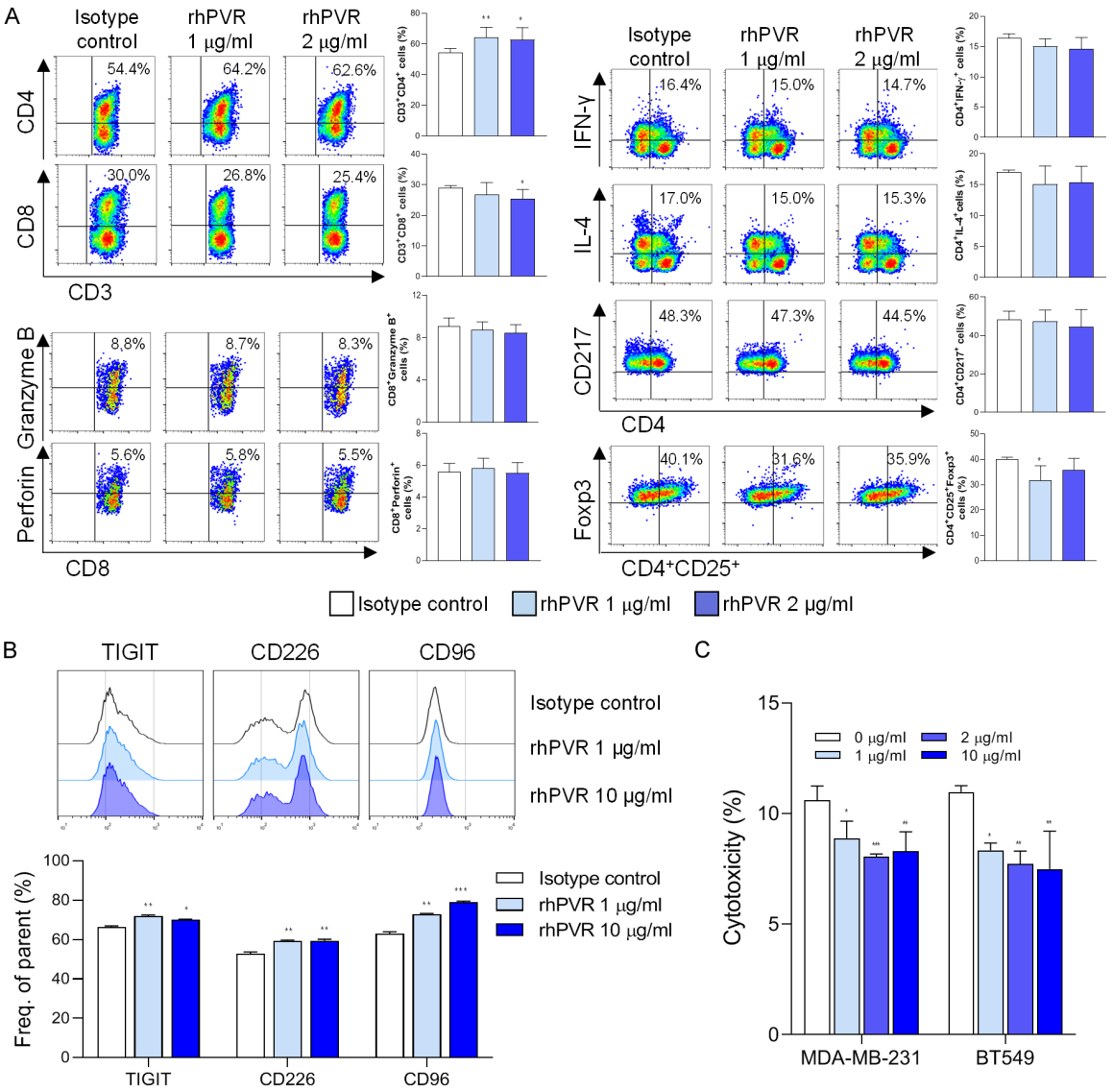

Figure 3. PVR increases CD4⁺ T cells. A. Human PBMC-derived CD3⁺ T cells were treated with human recombinant protein PVR (rhPVR; 1 and 2 μg/ml) for 24 h; T cell subtypes were analyzed via flow cytometry. B. PVR receptor expression, including TIGIT, CD226, and CD96, on T cells was investigated after 24-h rhPVR treatment. C. Quantification of T cell-mediated cytotoxicity against rhPVR-treated breast cancer cells using the nonradioactive LDH assay. Results are presented as mean ± SEM from three independent experiments.

tion in T cells, CTL responses were determined. *PVR* silencing significantly enriched CTL-mediated cytotoxicity in breast cancer cells, and radiation further increased tumor cell death (**Figure 2D**). Radiation-induced PVR expression was also observed in lung cancer cell lines, and knockdown of PVR increased the cytotoxicity of CTLs (Supplementary Figure 1D and 1E). Collectively, these findings suggest that PVR is a potential target for enhancing the efficacy of T cell-mediated immunotherapy against breast cancer.

PVR increases the CD4⁺ T cell population

To investigate the effect of PVR on T cell differentiation, CD3⁺ T cells were isolated from human PBMCs and treated with different doses of recombinant human PVR protein (rhPVR) for 24 h. **Figure 3A** demonstrates that PVR increased the proportion of CD3⁺CD4⁺ T cells but decreased that of CD3⁺CD8⁺ T cells; however, it did not affect T cell subsets such as Th1, Th2, Th17, and Treg cells. After rhPVR treatment, PVR receptor expression increased

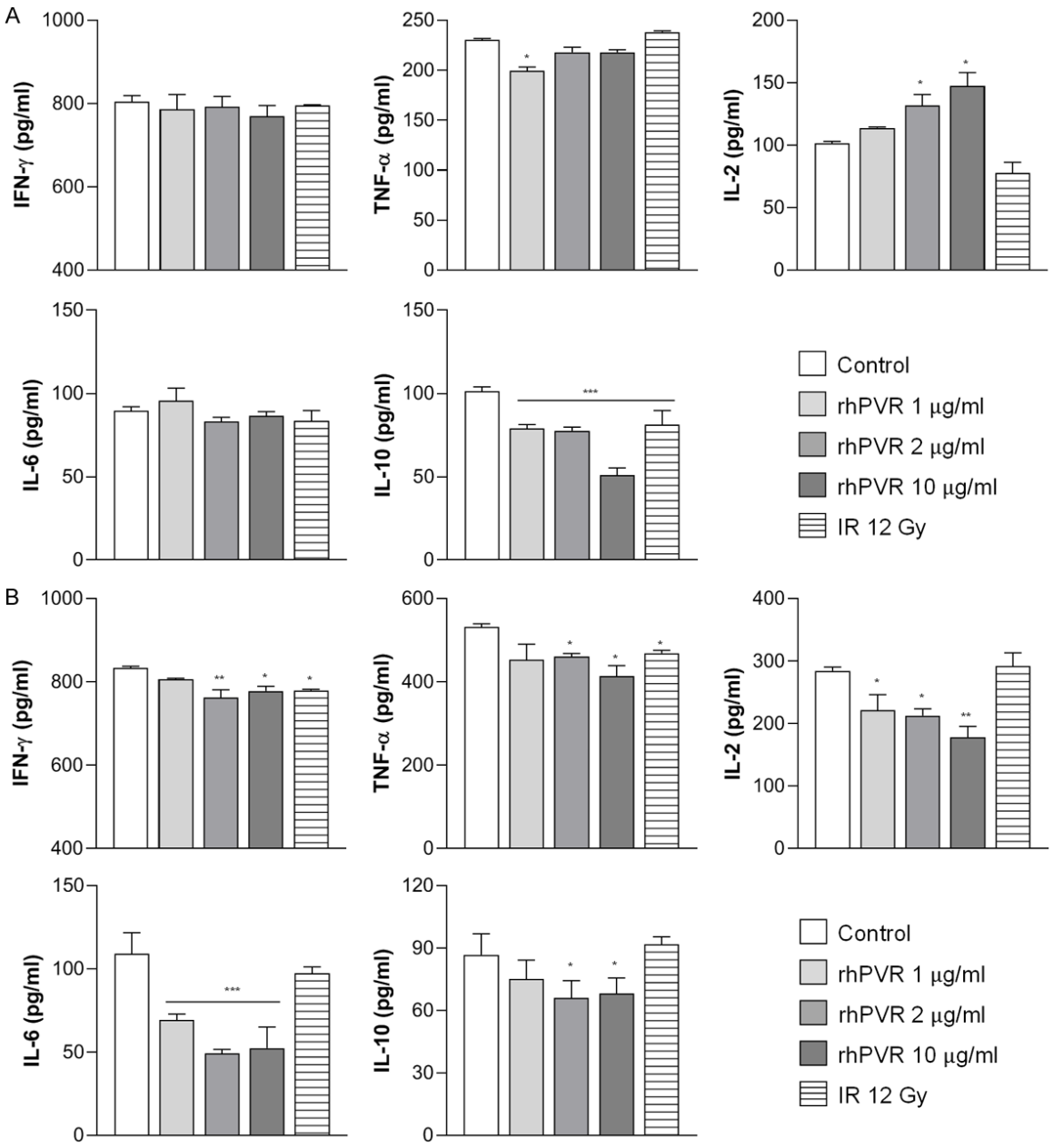

Figure 4. Effect of PVR-stimulated cancer cells on T cell-generated cytokine production. (A) MDA-MB-231 and (B) BT549 cells were treated with rhPVR or IR. The cells were co-cultured with T cells for 24 h. Cytokine release in T cell supernatants was quantified using ELISA kits. Results are presented as mean ± SEM from three independent experiments.

in T cells, including CD226, CD96, and TIGIT (**Figure 3B**). When TNBC cells were treated with rhPVR and CTL-mediated cytotoxicity was measured, there was a significant decrease in LDH release (**Figure 3C**). These results suggest that rhPVR treatment decreases the number of $CD8^+$ T cells and suppresses CTL-mediated antitumor activity.

PVR stimulation of cancer cells interferes with cytokine secretion

Because PVR is a negative IC, we investigated T cell-mediated cytokine secretion in co-cultured PVR-treated breast cancer cells. **Figure 4A** illustrates that after PVR treatment, the pro-inflammatory cytokines IFN-γ, TNF-α, and IL-6

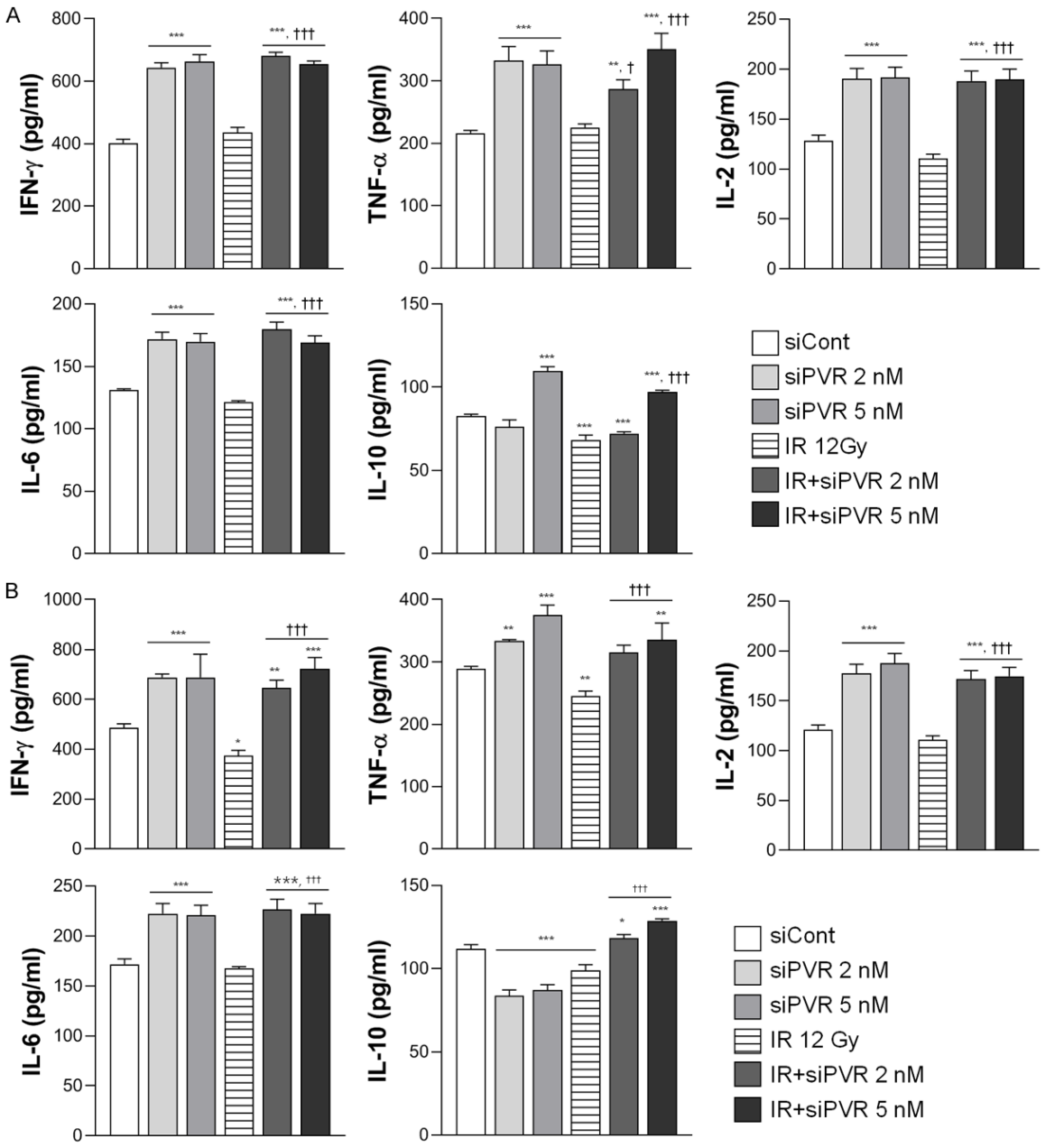

Figure 5. Effect of PVR-depleted cancer cells on T cell-generated cytokine production. (A) MDA-MB-231 and (B) BT549 cells were treated with siPVR and IR for 24 h. The cells were co-cultured with T cells for 72 h. Cytokines release in T cell supernatants were quantified using ELISA kits. Results are presented as mean ± SEM from three independent experiments. $^{*}P<0.05$, $^{**}P<0.01$, $^{***}P<0.001$ vs. Control, $^{\dagger}P<0.05$, $^{\dagger\dagger}P<0.01$, $^{\dagger\dagger\dagger}P<0.001$ vs. IR.

remained unchanged, whereas the anti-inflammatory cytokine IL-10 was decreased. IL-2, a growth and survival factor for T lymphocytes, was increased in MDA-MB-231 cells. However, both pro- and anti-inflammatory cytokine production was significantly decreased in co-cultured PVR-stimulated BT549 and T cells (**Figure 4B**). Furthermore, IR decreased IL-10 production alone in MDA-MB-231 cells, whereas IFN-γ and TNF-α generation was decreased in BT549 cells, indicating that radiation-induced immune responses depend on the cell types and contexts.

Next, we determined whether PVR suppression in tumors can restore cytokine secretion. **Figure 5A** and **5B** illustrate that PVR depletion significantly increased IFN-γ, TNF-α, IL-2, and IL-6 pro-

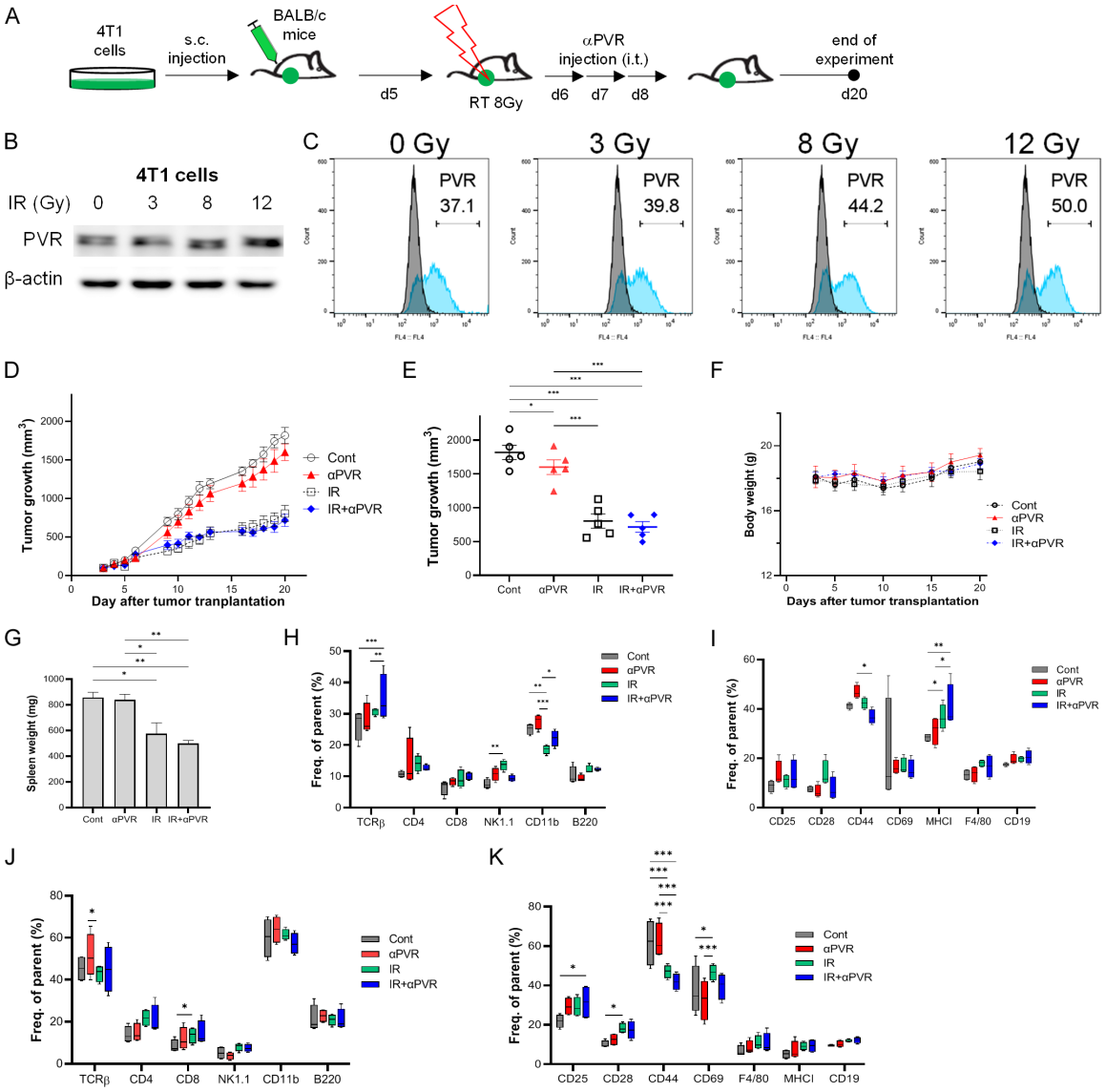

Figure 6. Anti-tumor efficacy of PVR inhibition in 4T1-bearing mice. (A) Scheme of the experiments. (B) Western blot analysis and (C) flow cytometry results of PVR expression in 4T1 cells 24 h after irradiation at various doses. (D) Monitoring of tumor growth in each experimental group. (E) Graphical representation of tumor volume at the end of the experiment. (F) Body weight change. (G) Spleen weight at the end of the experiment. (H, I) Subpopulation of immune cells and activation markers in spleen. (J, K) Subpopulation of immune cells and activation markers in TILs. Data represent means ± SEM of 5-6 mice per experiment. $^{*}P<0.05$, $^{**}P<0.01$, $^{***}P<0.001$.

duction in MDA-MB-231 and BT549 cells compared with control and irradiated cells. Furthermore, 5 nM siPVR increased IL-10 secretion in MDA-MB-231 but decreased it in BT549 cells. However, combined siPVR and irradiation treatment increased IL-10 production in both cell lines compared with irradiation alone. Collectively, these results suggest that PVR knockdown in cancer cells significantly increases cytokine production in co-cultured T cells. This capability is maintained in combined radiation treatment.

PVR blockade inhibits tumor growth in 4T1-bearing mice

To assess the antitumor effect of PVR inhibition, we used a syngeneic 4T1 murine TNBC transplanted model (**Figure 6A**). Similar to the data of human TNBC cells, PVR expression was markedly elevated by IR at the indicated dose in murine 4T1 cells (**Figure 6B** and **6C**). **Figure 6D** shows the tumor growth curves for the control, PVR blockade, IR alone, and IR + PVR blockade groups. Whereas PVR blockade alone

resulted in a significantly slower tumor growth than the control group, the combination of PVR blockade and IR did not further improve tumor control (**Figure 6D** and **6E**). To examine PVR-mediated systemic immunity, the subpopulation of immune cells in the spleen was analyzed via flow cytometry. While there were no body weight differences between all experimental groups, PVR blockade and/or IR significantly reduced spleen weight (**Figure 6F** and **6G**). Both PVR blockade with or without IR treatment increased T cells (TCRβ, CD3, and CD8) and myeloid cells (CD11b). In contrast to the increase in T cell numbers by PVR inhibition, the proportion of activated T cells (CD28 and CD44) did not increase. The increase in MHC I and F4/80 antigen-positive cells was consistent with the increased number of myeloid cells (**Figure 6H** and **6I**). We further examined the immune populations of TILs. Both CD4 and CD8 T cells were increased by PVR blockade with or without IR treatment, and PVR inhibition notably increased the population of activated T cells (**Figure 6J** and **6K**). An increase in the number of infiltrated myeloid cells was noticeable, but there was no difference between groups. Overall, PVR blockade enhanced the proportion of T cells and myeloid cells in the spleen as well as infiltrated and activated T cells in the TME.

Discussion

The role of RT as an immunomodulator has emerged as a novel and exciting concept. Many studies have reported that RT can cause cellular damage and activate the DNA damage response signaling pathway in tumors, inducing antigen presentation and leading to CTL priming [27, 28]. However, RT also exerts immunosuppressive effects [29, 30]. Recently, some studies have indicated that ICs act as immunosuppressors rather than immunoactivators in cancers. For example, tumor elimination by RT-activated immunity can be limited by negative Treg cell pathway activation, T cell exhaustion, and suppressive immune cell differentiation [31]. Preclinical animal models have revealed that PD-L1 expression can lead to RT resistance [8, 9]. Therefore, RT efficacy in the TME may be controversial, and the underlying mechanisms are largely unknown, thereby requiring comprehensive investigation.

In this study, we elucidated the role of PVR in breast cancer and its effect on T cell-mediated antitumor immune responses. PVR is an adhesion molecule belonging to the nectin-like family and is involved in various cancer-associated functions [12-14]. Although PVR was discovered >30 years ago, this multifunctional molecule has recently garnered scientific and clinical attention because its complex receptor interactions and related immune response functions remain uncharacterized. Moreover, PVR is often highly expressed in cancers, additionally increasing interest [12]. According to TCGA data, PVR is upregulated in colon, esophagus, head and neck, pancreas, rectum, and stomach cancers but not in breast cancer. However, among the breast cancer subtypes, PVR expression was significantly increased in TNBC and was highly correlated with poor OS. In addition, IR increased PVR upregulation in breast cancer cells, indicating its potential involvement in the sensitivity of radiation responses (**Figure 1**). Recent studies have reported that PVR is associated with cellular stress responses to reactive oxygen species (ROS) and is involved in the constitutive expression of *Myc*, with induction of the ATM-ATR DNA damage repair pathway in human tumor cell lines [32, 33]. Therefore, these findings suggest that RT increases PVR expression by inducing ROS and DNA damage in breast cancer.

To investigate whether PVR mediates RT resistance, cell viability and T cell-mediated cytotoxicity were determined in the presence and absence of PVR. PVR knockdown in breast cancer cells did not inhibit cell viability but enhanced CTL responses with or without IR (**Figure 2**). Consistent with our findings, Lee *et al*. have reported that PVR deletion increases the antitumor activity of $CD8^+$ T and NK cells in tumors [34]. Interestingly, irradiated tumor cells activated CTL responses compared with nonirradiated tumor cells; furthermore, CTL activity did not exert additive or synergistic effects on PVR suppression when combined with IR. Because IR simultaneously modulates various ICs in cancer cells, including PD-L1/L2, VISTA, HVEM, 4-1BBL, ICOSL, and PVR, outcomes may differ depending on cell types and context. Therefore, additional studies on the mechanism underlying radiation-induced PVR upregulation and verification of the combined effects of other ICs are warranted.

To date, many studies have reported that PVR binding to its receptors results in the expression of T cell-suppressive molecules and transfer of tumorigenic signals [21, 35]; furthermore, most studies have highlighted the importance of TIGIT [36, 37]. However, the direct effect of PVR on T cell function remains unclear. rhPVR treatment of T cells increased the proportion of $CD3^+CD4^+$ T cells but decreased that of $CD3^+CD8^+$ T cells, suggesting its role in decreasing T cell-mediated cytotoxicity. However, $CD4^+$ T cell differentiation into specific effector subtypes was not observed. Unfortunately, rhPVR treatment did not selectively increase the expression of the inhibitory TIGIT receptor but simultaneously increased the expression of all other receptors (**Figure 3**). PVR binds to CD226, resulting in a stimulatory immune response, whereas PVR binding to TIGIT and CD96 causes opposing immunosuppressive effects [38]. For example, TIGIT can inhibit NK cell-mediated immune responses by binding to PVR, thereby suppressing the antitumor effect of $CD8^+$ T cells [26]. Furthermore, the binding affinity of TIGIT to PVR is considerably higher than that of CD226 to PVR [39], indicating that suppressive immune responses outcompete positive immune activation. CD96 may act as an inhibitor in the dysfunctional phenotype in mouse tumor models, with NK cells producing higher IFN-γ in CD96 knockout mice. These mice exhibited resistance to experimental lung metastases and carcinogen-induced tumor development by activating $CD8^+$ T cells [21, 40, 41]. These inconsistent results may be attributed to the affinity and selectivity of rhPVR and limited in vitro experiments. Therefore, further studies with time and dose variations are warranted.

Because cytokines are important in regulating immune responses, we evaluated whether changes of PVR expression in tumors affect the cytokine-producing ability of T cells. Both pro- and anti-inflammatory cytokine secretion decreased in co-cultures of T cells and rhPVR-treated breast cancer cells (**Figure 4**). Furthermore, the activity of T cells cultured with rhPVR-treated BT549 cells was greater and clearer than that of MDA-MB-231 cells. However, in both cell lines, conflicting results were observed for IL-2 secretion. Because MDA-MB-231 cells are more radioresistant than BT549 cells, more or sustained IL-2-induced T cell proliferation is needed to destroy tumor cells. Compared with the cytokine profile by rhPVR-induced PVR upregulation, siPVR-treated PVR inhibition resulted in more distinct proinflammatory cytokine induction (**Figure 5**). However, similar to CTL responses, no additive or synergistic effects were observed when combined with radiation. These results indicate that radiation-increased PVR expression may play a minor role in the TME because PVR on tumors conveys both positive and negative signals, and can interact with other radiation-altered ICs.

We further confirmed that PVR blockade delayed tumor growth compared with that of the control group, but its combination with IR did not demonstrate synergistic antitumor effects (**Figure 6**). Previous studies demonstrated that loss of tumor-derived PVR expression reduced tumor progression and metastasis in cervical cancer [42], colon cancer [43], non-small cell lung cancer [34], and hepatocellular carcinoma [44]. Liu *et al.* reported that targeting PVR signaling by injecting C57BL/6 mice with PVR knockout cervical cells inhibited tumor progression in mice [42]. The depletion of PVR increased the level of infiltrating $CD8^+$ T lymphocytes in tissues and the secretion of IFN-γ and TNF-α. This is consistent with our results showing that anti-PVR antibody treatment significantly increased the proportion of T lymphocytes (TCRβ, CD4, and CD8 T cells) and myeloid cells in splenocytes and tumor tissues. The absence of effectiveness of combined IR and PVR blockade may be due to non-optimal treatment schedules, such as insufficient PVR blockade, inadequate RT dose, and nonideal sequence of PVR blockade administration. Nonetheless, we demonstrated that PVR knockdown in TNBC increased T cell-mediated antitumor activity by inducing proinflammatory cytokine secretion; this suggests that PVR functions as an inhibitory IC in addition to its previous role as a proto-oncogene [45], and may be an attractive target to overcome resistance against chemotherapy or radiotherapy.

Conclusion

Currently, many different PVR-targeting antitumor approaches have been investigated, including recombinant oncolytic polioviruses, monoclonal antibodies, and genetically engineered adoptive cell therapy. However, app-

roaches using anti-PVR antibodies remain scarce in preclinical and clinical trials because PVR expression patterns and kinetics remain unknown. Moreover, these approaches may provoke the unwanted inhibition of activating interactions and exert weaker effects than direct inhibitory receptor blockade. Although many aspects remain to be scrutinized, our study demonstrates that PVR induction in TNBC is a significant irradiation marker, making it a promising prognostic biomarker and therapeutic target. In the near future, IC inhibitors, DC vaccines, and adoptive cell therapies, which are emerging immunotherapies, can be used to target PVR for better clinical outcomes.

Acknowledgements

This work was supported by the National Research Foundation of Korea under grant number NRF-2020R1A2C1007138 and Korea Institute of Radiological and Medical Sciences under grant number 50531-2023, which was funded by the Korean government, Ministry of Science, and ICT.

Disclosure of conflict of interest

None.

Address correspondence to: Jie-Young Song, Division of Radiation Biomedical Research, Korea Institute of Radiological and Medical Sciences, 75 Nowon-ro, Nowon-gu, Seoul 01812, Republic of Korea. Tel: 8229701308; E-mail: immu@kirams.re.kr

References

[1] Ozpiskin OM, Zhang L and Li JJ. Immune targets in the tumor microenvironment treated by radiotherapy. Theranostics 2019; 9: 1215-1231.

[2] Shevtsov M, Sato H, Multhoff G and Shibata A. Novel approaches to improve the efficacy of immuno-radiotherapy. Front Oncol 2019; 9: 156.

[3] Demaria S, Coleman CN and Formenti SC. Radiotherapy: changing the game in immunotherapy. Trends Cancer 2016; 2: 286-294.

[4] Weichselbaum RR, Liang H, Deng L and Fu YX. Radiotherapy and immunotherapy: a beneficial liaison? Nat Rev Clin Oncol 2017; 14: 365-379.

[5] Formenti SC and Demaria S. Combining radiotherapy and cancer immunotherapy: a paradigm shift. J Natl Cancer Inst 2013; 105: 256-265.

[6] Burnette BC, Liang H, Lee Y, Chlewicki L, Khodarev NN, Weichselbaum RR, Fu YX and Auh SL. The efficacy of radiotherapy relies upon induction of type i interferon-dependent innate and adaptive immunity. Cancer Res 2011; 71: 2488-2496.

[7] Garcia-Diaz A, Shin DS, Moreno BH, Saco J, Escuin-Ordinas H, Rodriguez GA, Zaretsky JM, Sun L, Hugo W, Wang X, Parisi G, Saus CP, Torrejon DY, Graeber TG, Comin-Anduix B, Hu-Lieskovan S, Damoiseaux R, Lo RS and Ribas A. Interferon receptor signaling pathways regulating PD-L1 and PD-L2 expression. Cell Rep 2017; 19: 1189-1201.

[8] Deng L, Liang H, Burnette B, Beckett M, Darga T, Weichselbaum RR and Fu YX. Irradiation and anti-PD-L1 treatment synergistically promote antitumor immunity in mice. J Clin Invest 2014; 124: 687-695.

[9] Dovedi SJ, Adlard AL, Lipowska-Bhalla G, McKenna C, Jones S, Cheadle EJ, Stratford IJ, Poon E, Morrow M, Stewart R, Jones H, Wilkinson RW, Honeychurch J and Illidge TM. Acquired resistance to fractionated radiotherapy can be overcome by concurrent PD-L1 blockade. Cancer Res 2014; 74: 5458-5468.

[10] Voronova V, Vislobokova A, Mutig K, Samsonov M, Peskov K, Sekacheva M, Materenchuk M, Bunyatyan N and Lebedeva S. Combination of immune checkpoint inhibitors with radiation therapy in cancer: a hammer breaking the wall of resistance. Front Oncol 2022; 12: 1035884.

[11] Ribas A and Wolchok JD. Cancer immunotherapy using checkpoint blockade. Science 2018; 359: 1350-1355.

[12] Kucan Brlic P, Lenac Rovis T, Cinamon G, Tsukerman P, Mandelboim O and Jonjic S. Targeting PVR (CD155) and its receptors in anti-tumor therapy. Cell Mol Immunol 2019; 16: 40-52.

[13] Sloan KE, Stewart JK, Treloar AF, Matthews RT and Jay DG. CD155/PVR enhances glioma cell dispersal by regulating adhesion signaling and focal adhesion dynamics. Cancer Res 2005; 65: 10930-10937.

[14] Zhuo B, Li Y, Gu F, Li Z, Sun Q, Shi Y, Shen Y, Zhang F, Wang R and Wang X. Overexpression of CD155 relates to metastasis and invasion in osteosarcoma. Oncol Lett 2018; 15: 7312-7318.

[15] Xu Y, Cui G, Jiang Z, Li N and Zhang X. Survival analysis with regard to PD-L1 and CD155 expression in human small cell lung cancer and a comparison with associated receptors. Oncol Lett 2019; 17: 2960-2968.

[16] Fang L, Zhao F, Iwanowycz S, Wang J, Yin S, Wang Y and Fan D. Anticancer activity of emo-

din is associated with downregulation of CD155. Int Immunopharmacol 2019; 75: 105763.
[17] Zhang J, Zhu Y, Wang Q, Kong Y, Sheng H, Guo J, Xu J and Dai B. Poliovirus receptor CD155 is up-regulated in muscle-invasive bladder cancer and predicts poor prognosis. Urol Oncol 2020; 38: 41.e11-41.e18.
[18] Nishiwada S, Sho M, Yasuda S, Shimada K, Yamato I, Akahori T, Kinoshita S, Nagai M, Konishi N and Nakajima Y. Clinical significance of CD155 expression in human pancreatic cancer. Anticancer Res 2015; 35: 2287-2297.
[19] O'Donnell JS, Madore J, Li XY and Smyth MJ. Tumor intrinsic and extrinsic immune functions of CD155. Semin Cancer Biol 2020; 65: 189-196.
[20] Lupo KB and Matosevic S. CD155 immunoregulation as a target for natural killer cell immunotherapy in glioblastoma. J Hematol Oncol 2020; 13: 76.
[21] Chan CJ, Martinet L, Gilfillan S, Souza-Fonseca-Guimaraes F, Chow MT, Town L, Ritchie DS, Colonna M, Andrews DM and Smyth MJ. The receptors CD96 and CD226 oppose each other in the regulation of natural killer cell functions. Nat Immunol 2014; 15: 431-438.
[22] Song KH, Jung SY, Kang SM, Kim MH, Ahn J, Hwang SG, Lee JH, Lim DS, Nam SY and Song JY. Induction of immunogenic cell death by radiation-upregulated karyopherin alpha 2 in vitro. Eur J Cell Biol 2016; 95: 219-227.
[23] Song KH, Jung SY, Park JI, Ahn J, Park JK, Um HD, Park IC, Hwang SG, Ha H and Song JY. Inhibition of Karyopherin-alpha2 augments radiation-induced cell death by perturbing BRCA1-mediated DNA repair. Int J Mol Sci 2019; 20: 2843.
[24] Song KH, Kim MH, Kang SM, Jung SY, Ahn J, Woo HJ, Nam SY, Hwang SG, Ryu SY and Song JY. Analysis of immune cell populations and cytokine profiles in murine splenocytes exposed to whole-body low-dose irradiation. Int J Radiat Biol 2015; 91: 795-803.
[25] Yoshikawa K, Ishida M, Yanai H, Tsuta K, Sekimoto M and Sugie T. Immunohistochemical analysis of CD155 expression in triple-negative breast cancer patients. PLoS One 2021; 16: e0253176.
[26] Lepletier A, Madore J, O'Donnell JS, Johnston RL, Li XY, McDonald E, Ahern E, Kuchel A, Eastgate M, Pearson SA, Mallardo D, Ascierto PA, Massi D, Merelli B, Mandala M, Wilmott JS, Menzies AM, Leduc C, Stagg J, Routy B, Long GV, Scolyer RA, Bald T, Waddell N, Dougall WC, Teng MWL and Smyth MJ. Tumor CD155 expression is associated with resistance to anti-PD1 immunotherapy in metastatic melanoma. Clin Cancer Res 2020; 26: 3671-3681.
[27] Golden EB, Pellicciotta I, Demaria S, Barcellos-Hoff MH and Formenti SC. The convergence of radiation and immunogenic cell death signaling pathways. Front Oncol 2012; 2: 88.
[28] Green DR, Ferguson T, Zitvogel L and Kroemer G. Immunogenic and tolerogenic cell death. Nat Rev Immunol 2009; 9: 353-363.
[29] Ruckert M, Flohr AS, Hecht M and Gaipl US. Radiotherapy and the immune system: more than just immune suppression. Stem Cells 2021; 39: 1155-1165.
[30] Wennerberg E, Lhuillier C, Vanpouille-Box C, Pilones KA, Garcia-Martinez E, Rudqvist NP, Formenti SC and Demaria S. Barriers to radiation-induced in situ tumor vaccination. Front Immunol 2017; 8: 229.
[31] Lan J, Li R, Yin LM, Deng L, Gui J, Chen BQ, Zhou L, Meng MB, Huang QR, Mo XM, Wei YQ, Lu B, Dicker A, Xue JX and Lu Y. Targeting myeloid-derived suppressor cells and programmed death ligand 1 confers therapeutic advantage of ablative hypofractionated radiation therapy compared with conventional fractionated radiation therapy. Int J Radiat Oncol Biol Phys 2018; 101: 74-87.
[32] Ardolino M, Zingoni A, Cerboni C, Cecere F, Soriani A, Iannitto ML and Santoni A. DNAM-1 ligand expression on Ag-stimulated T lymphocytes is mediated by ROS-dependent activation of DNA-damage response: relevance for NK-T cell interaction. Blood 2011; 117: 4778-4786.
[33] Fionda C, Abruzzese MP, Zingoni A, Soriani A, Ricci B, Molfetta R, Paolini R, Santoni A and Cippitelli M. Nitric oxide donors increase PVR/CD155 DNAM-1 ligand expression in multiple myeloma cells: role of DNA damage response activation. BMC Cancer 2015; 15: 17.
[34] Lee BR, Chae S, Moon J, Kim MJ, Lee H, Ko HW, Cho BC, Shim HS, Hwang D, Kim HR and Ha SJ. Combination of PD-L1 and PVR determines sensitivity to PD-1 blockade. JCI Insight 2020; 5: e128633.
[35] Feng S, Isayev O, Werner J and Bazhin AV. CD96 as a potential immune regulator in cancers. Int J Mol Sci 2023; 24: 1303.
[36] Wang F, Liu S, Liu F, Xu T, Ma J, Liang J, Wang J, Liu D, Yang F, Li J and Xing N. TIGIT immune checkpoint blockade enhances immunity of human peripheral blood NK cells against castration-resistant prostate cancer. Cancer Lett 2023; 568: 216300.
[37] Ge Z, Peppelenbosch MP, Sprengers D and Kwekkeboom J. TIGIT, the next step towards successful combination immune checkpoint therapy in cancer. Front Immunol 2021; 12: 699895.
[38] Stamm H, Oliveira-Ferrer L, Grossjohann EM, Muschhammer J, Thaden V, Brauneck F,

Kischel R, Muller V, Bokemeyer C, Fiedler W and Wellbrock J. Targeting the TIGIT-PVR immune checkpoint axis as novel therapeutic option in breast cancer. Oncoimmunology 2019; 8: e1674605.

[39] Lozano E, Dominguez-Villar M, Kuchroo V and Hafler DA. The TIGIT/CD226 axis regulates human T cell function. J Immunol 2012; 188: 3869-3875.

[40] Mittal D, Lepletier A, Madore J, Aguilera AR, Stannard K, Blake SJ, Whitehall VLJ, Liu C, Bettington ML, Takeda K, Long GV, Scolyer RA, Lan R, Siemers N, Korman A, Teng MWL, Johnston RJ, Dougall WC and Smyth MJ. CD96 is an immune checkpoint that regulates CD8(+) T-cell antitumor function. Cancer Immunol Res 2019; 7: 559-571.

[41] Lepletier A, Lutzky VP, Mittal D, Stannard K, Watkins TS, Ratnatunga CN, Smith C, McGuire HM, Kemp RA, Mukhopadhyay P, Waddell N, Smyth MJ, Dougall WC and Miles JJ. The immune checkpoint CD96 defines a distinct lymphocyte phenotype and is highly expressed on tumor-infiltrating T cells. Immunol Cell Biol 2019; 97: 152-164.

[42] Liu L, Wang A, Liu X, Han S, Sun Y, Zhang J, Guo L and Zhang Y. Blocking TIGIT/CD155 signalling reverses CD8(+) T cell exhaustion and enhances the antitumor activity in cervical cancer. J Transl Med 2022; 20: 280.

[43] Zheng Q, Wang B, Gao J, Xin N, Wang W, Song X, Shao Y and Zhao C. CD155 knockdown promotes apoptosis via AKT/Bcl-2/Bax in colon cancer cells. J Cell Mol Med 2018; 22: 131-140.

[44] Jin AL, Zhang CY, Zheng WJ, Xian JR, Yang WJ, Liu T, Chen W, Li T, Wang BL, Pan BS, Li Q, Cheng JW, Wang PX, Hu B, Zhou J, Fan J, Yang XR and Guo W. CD155/SRC complex promotes hepatocellular carcinoma progression via inhibiting the p38 MAPK signalling pathway and correlates with poor prognosis. Clin Transl Med 2022; 12: e794.

[45] Gao J, Zheng Q, Xin N, Wang W and Zhao C. CD155, an onco-immunologic molecule in human tumors. Cancer Sci 2017; 108: 1934-1938.

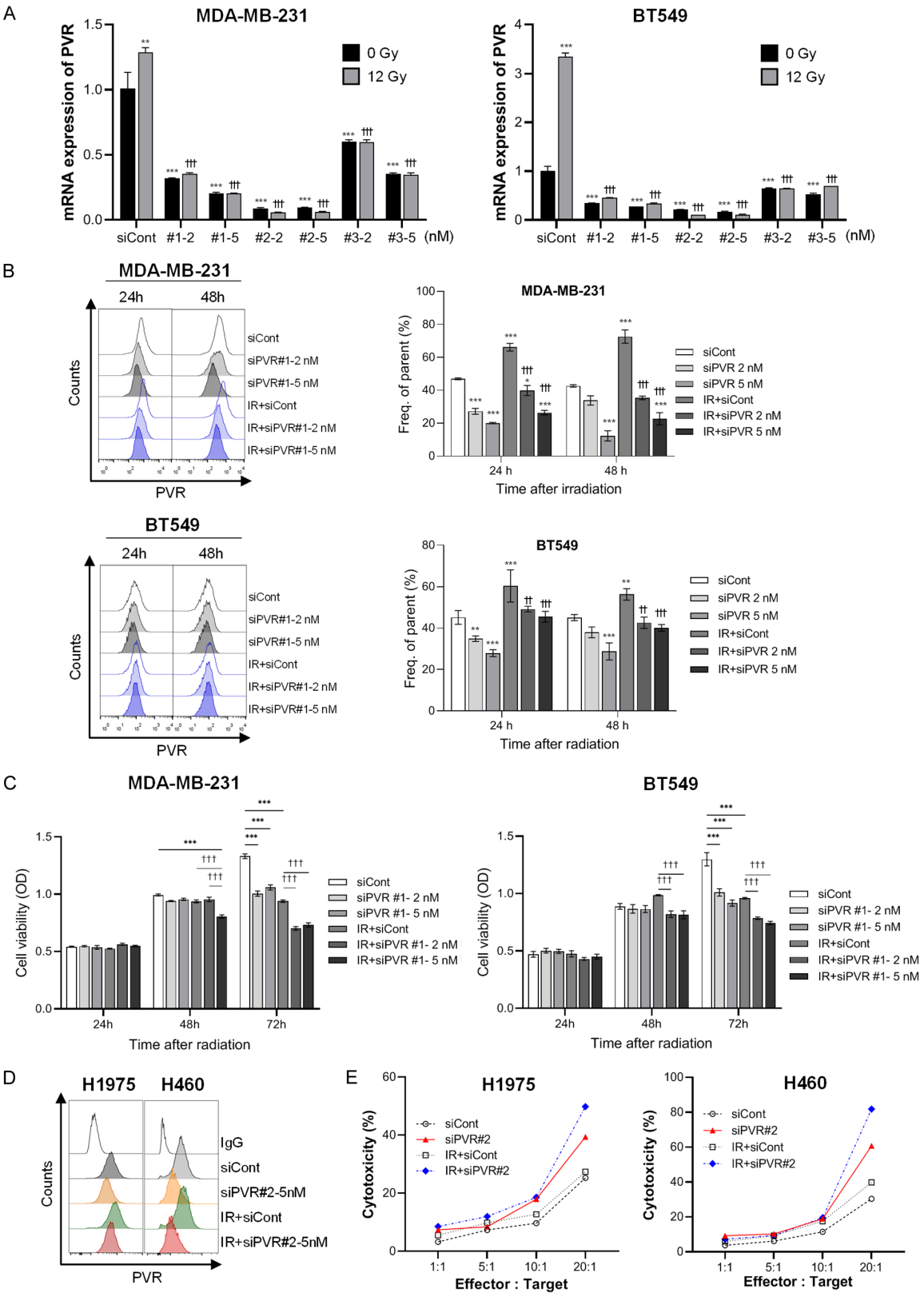

Supplementary Figure 1. Evaluation of the efficacy of siPVRs. A. Breast cancer cells were transfected with 2 and 5 nM of three types of siPVRs (#1, #2, or #3) and irradiated with 12 Gy. PVR expression was determined using RT-PCR analysis 24 h after IR. B. Breast cancer cells were transfected with siPVR#1 (2 and 5 nM). PVR expression was detected at 24-48 h after IR using flow cytometry. C. Cell viability was examined using the MTT assay. D. H1975 and H460 lung cancer cells were transfected with 5 nM of siPVR#2. PVR expression was determined at 24 h after IR using flow cytometry. E. CTL-mediated lung cancer cell killing was measured using the nonradioactive LDH assay. $^{*}P<0.05$, $^{**}P<0.01$, $^{***}P<0.001$ vs. siCont, $^{\dagger}P<0.05$, $^{\dagger\dagger}P<0.01$, $^{\dagger\dagger\dagger}P<0.001$ vs. IR+siCont.